**Prolonged Continuous Monitoring of Regional Lung Function in Infants with Respiratory Failure**

Tobias H. Becher (1); Martijn Miedema (2); Merja Kallio (3); Thalia Papadouri (4); Christina Karaoli (4); Louiza Sophocleous (5); Marika Rahtu (3); Ruud W. van Leuteren (2); Andreas D. Waldmann (6, 11); Claas Strodthoff (1); Rebecca Yerworth (7); Antoine Dupré (8); Mohamed-Rida Benissa (8); Sven Nordebo (9); Davood Khodadad (9); Richard Bayford (10); Roseanne Vliegenthart (2); Peter C. Rimensberger (8); Anton H. van Kaam (2); Inéz Frerichs (1)

1) Department of Anesthesiology and Intensive Care Medicine, University Medical Center Schleswig- Holstein, Campus Kiel, Germany
2) Department of Neonatology, Emma Children's Hospital, Amsterdam University Medical Centers, University of Amsterdam and Vrije Universiteit Amsterdam, Amsterdam, Netherlands
3) PEDEGO Research Unit, Medical Research Center Oulu, University of Oulu, and Department of Children and Adolescents, Oulu University Hospital, Oulu, Finland
4) Department of Neonatology, Archbishop Makarios III Hospital, Nicosia, Cyprus
5) Department of Electrical and Computer Engineering, University of Cyprus, Nicosia, Cyprus
6) SenTec AG (formerly Swisstom AG), Landquart, Switzerland
7) Department of Medical Physics and Biomedical Engineering, University College London, United Kingdom;
8) Division of Neonatology and Paediatric Intensive Care, Department of Paediatrics, University Hospital of Geneva, University of Geneva, Switzerland
9) Department of Physics and Electrical Engineering, Linnaeus University, Växjö, Sweden
10) Department of Natural Sciences, Middlesex University, London, United Kingdom
11) Department of Anesthesiology and Intensive Care Medicine, Rostock University Medical Center, Rostock, Germany

**Corresponding author contact information**

Tobias Becher
Department of Anesthesiology and Intensive Care Medicine
University Medical Center Schleswig- Holstein, Campus Kiel
Arnold-Heller-Straße 3, Haus R3
D-24105 Kiel
Germany
E-Mail: tobias.becher@uksh.de
Phone: +49 431 500 20980 Fax: +49 431 500 20804

ANNALSATS Articles in Press. Published December 13, 2021 as 10.1513/AnnalsATS.202005-562OC

**Authors´ contributions: Conception and design:** T.H.B., R.B., A.H.v.K., R.Y., P.C.R., I.F.; **Data acquisition:** M.K., M.M., M.R., R.W.v.L., C.K., T.P., L.S., R.V., A.H.v.K.; **Analysis and interpretation of data**: T.H.B., M.M., M.K., M.R., L.S., A.D.W., C.S., R.Y., A.D., M.R.B., S.N., D.K., R.B., I.F.; **Drafting the manuscript for important intellectual content:** T.H.B., M.M., M.K., M.R., L.S., A.D.W., C.S., R.Y., A.D., M.R.B., P.C.R., A.H.v.K., I.F. **Revision and final approval of the manuscript:** All authors

**Sources of funding:** This study has received funding from the European Union's Horizon 2020 Research and Innovation Programme under grant agreement No. 668259 and by the Swiss State Secretariat for Education, Research and Innovation (SERI) under contract number 15.0342-1. Dr Kallio was funded by the Finnish Foundation for Pediatric Research.

**Running title:** EIT for continuous monitoring in neonatal and pediatric intensive care

**Subject category:** 4.11 Pediatric Critical Care

**Word count:** 3402

This article has an online data supplement, which is accessible from this issue's table of content online at www.atsjournals.org

ANNALSATS Articles in Press. Published December 13, 2021 as 10.1513/AnnalsATS.202005-562OC

**Abstract**

**Rationale:** Electrical impedance tomography (EIT) allows instantaneous and continuous visualization of regional ventilation and changes in end-expiratory lung volume at the bedside. There is particular interest in using EIT for monitoring in critically ill neonates and young children with respiratory failure. Previous studies have focused only on short-term monitoring in small populations. The feasibility and safety of prolonged monitoring with EIT in neonates and young children has not been demonstrated yet.

**Objectives:** To evaluate the feasibility and safety of long-term EIT monitoring in a routine clinical setting and to describe changes in ventilation distribution and homogeneity over time and with positioning in a multi-center cohort of neonates and young children with respiratory failure.

**Methods:** At four European University Hospitals, we conducted an observational study (NCT02962505) on 200 patients with post-menstrual ages (PMA) between 25 weeks and 36 months, at risk for or suffering from respiratory failure. Continuous EIT data were obtained using a novel textile 32-electrode interface and recorded at 48 images/s for up to 72 hours. Clinicians were blinded to EIT images during the recording. EIT parameters and the effects of body position on ventilation distribution were analyzed offline.

**Results:** The average duration of EIT measurements was 53±20 hours. Skin contact impedance was sufficient to allow image reconstruction for valid ventilation analysis during 92[77-98]% (median[interquartile range]) of examination time. EIT examinations were well tolerated, with minor skin irritations (temporary redness or imprint) occurring in 10% of patients and no moderate or severe adverse events. Higher ventilation amplitude was found in the dorsal and

ANNALSATS Articles in Press. Published December 13, 2021 as 10.1513/AnnalsATS.202005-562OC

right lung areas when compared with the ventral and left regions respectively. Prone positioning resulted in an increase in the ventilation-related EIT signal in the dorsal hemithorax, indicating increased ventilation of the dorsal lung areas. Lateral positioning led to a redistribution of ventilation towards the dependent lung in preterm infants and to the non-dependent lung in patients with PMA above 37 weeks.

**Conclusions:** EIT allows continuous long-term monitoring of regional lung function in neonates and young children for up to 72 hours with minimal adverse effects. Our study confirmed the presence of posture-dependent changes in ventilation distribution and their dependency on PMA in a large patient cohort.

Clinical trial registered with ClinicalTrials.gov (NCT02962505)

ANNALSATS Articles in Press. Published December 13, 2021 as 10.1513/AnnalsATS.202005-562OC

Electrical impedance tomography (EIT) is a functional imaging modality that allows instantaneous and continuous visualization of regional ventilation and changes in end-expiratory lung volume at the bedside. By virtue of its non-invasive design and the absence of radiation, there is a special interest in the application of EIT in neonates and young children with respiratory failure (1,2). Previous studies have shown that EIT can identify areas of (recruitable) alveolar collapse and overdistension in this patient population (3, 4) and demonstrated the usefulness of EIT in guiding ventilator settings during both invasive and non-invasive modes of respiratory support (5, 6). In preterm infants, EIT can be used to analyze the pressure-volume relationship of the respiratory system (4, 7) and to monitor the changes in lung volume and ventilation following changes in positioning (8-13) and surfactant treatment (14-16). EIT also has the potential to identify adverse events like pneumothorax (17-20), atelectasis (21) and endotracheal tube malposition (22, 23). These results imply that EIT may be suitable for continuous real-time monitoring of regional lung function, for rapid detection of adverse respiratory events and potentially for guiding therapy and interventions at the bedside.

In previous studies in the neonatal and pediatric population, EIT examinations were limited both in scope and duration, examining single prespecified events or interventions within a time period of typically less than one hour (6-9, 25). These, mostly single center, studies were carried out under controlled conditions with highly trained researchers continuously present at the bedside and other care procedures were paused during the EIT examinations. Most previous studies used single adhesive electrodes, that had to be attached manually around the patients' chest circumference in one transverse plane. Recently, a novel textile 32-electrode

ANNALSATS Articles in Press. Published December 13, 2021 as 10.1513/AnnalsATS.202005-562OC

interface for neonatal and pediatric EIT examination has been developed, which facilitates use of EIT in daily practice and allows prolonged periods of EIT examination (25).

Although none of the previous studies reports any complications or adverse events associated with EIT monitoring, data on the feasibility and safety of prolonged monitoring with EIT in neonates and young children are missing (1).Within the Continuous Regional Analysis Device for neonate Lungs (CRADL) project, we conducted a prospective observational study (ClinicalTrials.gov Identifier: NCT02962505) with the aim of investigating the feasibility of continuous EIT monitoring and of providing data on ventilation distribution and homogeneity using a non-adhesive textile electrode belt in neonates and young children of up to 36 months postmenstrual age (PMA) during real-life clinical conditions.

## Methods

We conducted a multi-center prospective observational study including neonates and children treated in the neonatal or pediatric intensive care unit (NICU/PICU) who had respiratory failure or who were considered being “at risk” for developing respiratory failure. Exclusion criteria were PMA<25 weeks, body weight <600 g and thorax skin lesions. The protocol was approved by the local ethics committees and written informed consent was obtained from both parents. EIT examinations were carried out with the SenTec BB$^2$ system using non-adhesive textile 32-electrode belts for neonatal and pediatric use (SenTec AG (formerly Swisstom AG), Landquart, Switzerland). The belts were placed on the patients´ chest circumference along the 5$^{th}$ to 6$^{th}$ intercostal space using neonatal ultrasound gel (Aquasonic 100, Parker Laboratory, USA) as

ANNALSATS Articles in Press. Published December 13, 2021 as 10.1513/AnnalsATS.202005-562OC

an electrolyte to improve electrode-skin contact. The EIT device was equipped with a study-specific graphical user interface (GUI) that blinded the clinician users to the EIT images. This GUI enabled the purely observational character of the study. The GUI provided information on the quality of electrode contact impedance to allow reattaching the belt or reapplying the ultrasound gel if necessary. The GUI furthermore allowed documentation of clinical interventions and findings in real time. In addition to EIT data, a video log was recorded for continuous monitoring of patient position and interventions. Figure 1 shows the EIT device with its study-specific GUI in a clinical setting with the EIT belt placed around the infant's chest circumference.

Study data acquisition was carried out for up to 72 hours, which equaled the maximum permitted duration of EIT belt application by the time the study was conceived. Data acquisition was terminated earlier if the patient was discharged from the NICU/PICU, required surgical interventions or at the parents' request, who in some cases decided a priori to give consent for only 24 or 48 hours of EIT data acquisition.

Following data collection, off-line image reconstruction was performed with the device's built-in image reconstruction algorithm based on the Graz consensus Reconstruction algorithm for EIT (26). Time points of end-inspiration and end-expiration were detected with a breath detection algorithm optimized for neonates and young infants (27). Ventilation inhomogeneity was quantified with the global inhomogeneity index (GI index (28)) and the coefficient of variation (29). Ventral-to-dorsal and right-to-left ventilation distributions were assessed by calculating the fraction of ventilation (1) in the ventral, dorsal, right and left hemithoraces.

ANNALSATS Articles in Press. Published December 13, 2021 as 10.1513/AnnalsATS.202005-562OC

The primary endpoint was the proportion of EIT examination time suitable for analyzing, which was defined as the percentage of EIT examination time with at least 26 out of 32 sensors exhibiting a skin contact impedance of < 700 Ohm (the threshold required for image reconstruction by the Sentec $BB^2$ system used in the study). The secondary outcome measures were changes in the abovementioned EIT parameters over time and changes in ventilation distribution induced by confirmed changes in patient position (figure 2). Skin condition was checked routinely during patient care by the clinical staff. Changes in skin condition as well as other adverse events were documented on paper-based case report forms.

Due to the feasibility character of the study and the lack of data on adverse effects of EIT in the literature, no sample size calculation with respect to adverse effects was performed a priori.

Data were tested for normal distribution using the Shapiro-Wilk test. Normally and non-normally distributed values are presented as mean ± standard deviation and median ± interquartile range (IQR), respectively. Intraindividual comparisons were performed with One-Way-ANOVA for repeated measures, Friedman test, two-sided paired t-test or Wilcoxon matched pairs test, as appropriate. Interindividual comparisons were performed with One-Way-ANOVA, Kruskal-Wallis test, two-sided unpaired t-test or Mann-Whitney test, as appropriate. A *p*-value less than 0.05 was considered statistically significant. Statistical analysis was performed with GraphPad Prim 5.0 (GraphPad Software, La Jolla California, USA).

Additional details on EIT image acquisition and data analysis as well as explanations of EIT parameters are provided in an online supplement.

ANNALSATS Articles in Press. Published December 13, 2021 as 10.1513/AnnalsATS.202005-562OC

## Results

A total of 200 patients with a median PMA of 33 (IQR: 30-37, min-max: 25-159) weeks and weight of 1.6 (IQR: 1.2-2.8, min-max: 0.73-12.8) kg were included at four NICUs and one PICU: Amsterdam University Medical Centers, locations Academic Medical Center (n=79 patients included) and VU Medical Center (n=9), both Amsterdam, The Netherlands; Archbishop Makarios III Hospital, Nicosia, Cyprus (n=42) and Oulu University Hospital, Oulu, Finland (n=70). All patients included underwent full EIT data analysis (Figure 3). The population included 155 individuals with PMA (at time of study inclusion) of less than 37 weeks and 45 individuals with PMA above 37 weeks. The main causes for (imminent) respiratory failure were respiratory distress syndrome (n = 78), prematurity (n=66), transient tachypnea of the newborn (n=11), meconium aspiration (n = 11), bronchopulmonary dysplasia (n=10), bronchiolitis/obstructive bronchitis (n=6), pneumonia (n=6), persistent pulmonary hypertension (n=3) and others (n=9). The modes of respiratory support as well as information on fraction of inspired oxygen ($FiO_2$) and peripheral oxygen saturation ($SpO_2$) at the beginning and the end of the study are presented in table 1.

Skin contact impedance was sufficient to allow EIT image reconstruction during a median of 92 [77-98] % of examination time. The median duration of EIT recording was 58 [39-71] hours per patient. The median number of EIT belt manipulations documented using the study GUI was 1 per 24 hours of EIT recordings [IQR 0-3, Min-Max 0-11]. Similarly, the median number of ultrasound gel applications to improve electrode contact was 1 per 24 hours [IQR 0-1, Min-Max 0-8]. No moderate or serious study-related adverse events were observed. In one

ANNALSATS Articles in Press. Published December 13, 2021 as 10.1513/AnnalsATS.202005-562OC

patient, a minor imprint of the EIT belt on the skin was observed, which led to discontinuation of EIT monitoring 64 hours after study inclusion. The skin finding resolved spontaneously without further intervention. Transient redness of skin was observed in 20 patients in total, sometimes requiring belt readjustments or reapplication of contact agent but no further interventions.

The dorsal percentage of ventilation at baseline was 57.5±9.5% (noninvasive respiratory support: 58.5±8.8%; invasive respiratory support: 54.7±10.8%, p=0.01 vs. non-invasive) and did not change significantly during the study period. The right lung accounted for 55.6±13.9% (non-invasive: 56.4±13.1; invasive: 53.7±15.7; p=0.22) of tidal ventilation at baseline. This was more pronounced at the end of study recordings with 58.4±15.4% of tidal ventilation distributed to the right lung (p=0.03 in comparison to baseline). A summary of EIT parameters obtained in the whole study population is provided in table 2 showing that in general, measures of ventilation distribution and inhomogeneity were consistent over time with no significant changes during the study duration. We found no differences in right-to-left ventilation distribution but a higher dorsal fraction of ventilation in the subgroup of infants with PMA below 37 weeks in comparison to older infants. The baseline EIT parameters for the groups with PMA below and above 37 weeks are presented separately in supplementary table S1.

**Influence of positioning on EIT findings**

We found a small but statistically significant increase in the dorsal fraction of ventilation with prone positioning, indicating increased ventilation of the dorsal lung areas in the prone position as compared to the supine position. Note that “dorsal fraction of ventilation” refers to the

ANNALSATS Articles in Press. Published December 13, 2021 as 10.1513/AnnalsATS.202005-562OC

anatomically dorsal part of the lung, which is dependent in the supine position and non-dependent in the prone position. The dorsal redistribution of ventilation in the prone position was more pronounced in patients with PMA ≥ 37 weeks and less pronounced in premature infants with PMA < 37 weeks.

Comparing ventilation distribution between the right and left lateral position in the whole study population, we found no significant changes in right-to-left ventilation distribution. However, in the subgroup of infants with PMA < 37 weeks, lateral positioning led to significant redistributions of ventilation towards the dependent hemithorax. The opposite phenomenon was found in the subgroup with PMA ≥ 37 weeks: In these non-premature patients, lateral positioning led to a predominant redistribution of ventilation towards the non-dependent hemithorax (table 4).

Separate analyses of positioning for the subgroups of infants with prematurity, RDS, BPD and bronchiolitis as well as for invasive vs. non-invasive respiratory support are presented in supplementary tables S1, S2 and S3.

## Discussion

In this prospective observational study including 200 neonates and critically ill children, we demonstrated that monitoring of this group of patients with EIT for up to 72 hours is feasible and not associated with any significant adverse effects. During the study, we purposefully blinded clinicians to the EIT images to ensure that no clinical decisions would be taken based on these images by staff inexperienced in EIT image interpretation. Despite this blinding of bedside

ANNALSATS Articles in Press. Published December 13, 2021 as 10.1513/AnnalsATS.202005-562OC

staff to the EIT images, we were able to generate sufficient electrode contact impedance to allow EIT image reconstruction during a median of 92% of EIT examination time. These results were obtained in a real-life clinical setting, with different nurses and physicians using the equipment with only a few basic instructions. It is likely that the percentage of EIT examination time with sufficient electrode contact to allow image reconstruction will increase further when, in future studies and clinical EIT application, nurses and physicians will no longer be blinded to the reconstructed EIT images and become more experienced over time.

EIT examinations with the novel textile 32 electrode belt were generally well tolerated, with minor skin alterations occurring in about 10% of patients and only one case where this led to premature termination of EIT examinations. These results support the notion of EIT being an innocuous imaging modality suitable for continuous monitoring of regional lung function even in very preterm infants.

**Assessment of regional ventilation distribution with EIT**

Our analyses of regional ventilation distribution with EIT confirm previous findings of a higher ventilation amplitude in the dorsal lung areas as compared to the ventral lung areas and in the right lung as compared to the left lung (9, 10). The dorsal predominance of ventilation distribution was more pronounced in premature infants with PMA < 37 weeks as compared to older patients and in non-invasive ventilation as compared to invasive ventilation (supplementary table S3). In a cohort of forty stable preterm infants during non-invasive respiratory support, Thomson et al. found greater ventilation in the right lung, which is in line with our findings, and, in contrast to our findings, greater ventilation in the gravity non-

ANNALSATS Articles in Press. Published December 13, 2021 as 10.1513/AnnalsATS.202005-562OC

dependent lung (30). This discrepancy may be explained by the different EIT measures used in both studies: our study used the dorsal percentage of ventilation for assessing anteroposterior ventilation distribution. This was calculated by splitting the EIT image at one horizontal line in the middle of the anteroposterior thorax diameter and dividing the sum of tidal impedance changes within the dorsal hemithorax by the sum of tidal impedance changes within the thorax. In contrast, Thompson et al. calculated the difference between actual and "ideal" center of ventilation as calculated by the analysis software ibeX (Sentec, Landquart, Switzerland). The ideal center of ventilation calculated by ibex is 55% for supine position, which is similar to our findings.

Analyzing the effects of positioning on ventilation distribution, we found that prone positioning led to increased ventilation of the dorsal lung areas in the prone position as compared to the supine position, while lateral positioning resulted in no significant differences in right-to-left ventilation distribution when the whole study population was evaluated.

The dorsal redistribution of ventilation with prone positioning was more pronounced in infants with PMA above 37 weeks. These older patients also exhibited a significant redistribution of ventilation towards the non-dependent lung during lateral positioning. These findings are in contrast with previous studies demonstrating a reversal of the adult pattern of ventilation redistribution with positioning in non-premature infants (31, 32). A cross-sectional study investigating positional changes of ventilation distribution with EIT that included 55 healthy, spontaneously breathing, unsedated children between the ages of 6 months and 9 years demonstrated mixed results: 35% of participants showed consistently greater ventilation in the non-dependent lung, 15% showed consistently greater ventilation in the dependent lung

ANNALSATS Articles in Press. Published December 13, 2021 as 10.1513/AnnalsATS.202005-562OC

and the majority (51%) showed a varied pattern (33). Rehan et al examined the diaphragm resting length and shortening at the level of the zone of apposition between the supine and prone postures in 16 healthy term infants. In the prone position the diaphragm was thicker and the shortening greater (34). The general pattern of redistribution of ventilation towards the non-dependent lungs in infants with PMA above 37 weeks may be due to changes in gravity-dependent compression of the dependent hemidiaphragm.

In premature infants with PMA below 37 weeks, the redistribution of ventilation towards the dorsal lung areas with prone positioning was less pronounced than in older patients. Lateral positioning led to a redistribution of ventilation towards the dependent lung in these preterm infants, in contrast to the redistribution towards the non-dependent lung we observed in patients with PMA above 37 weeks.

Some previous studies comparing ventilation distribution between different body positions in neonates showed no difference in ventilation distribution with positioning (10, 12) whereas other studies demonstrated a shift in ventilation towards the dependent lung regions after positioning (11, 13). In a group of 20 preterm infants recovering from respiratory disease, Wolfson et al found an improvement in thoracoabdominal synchrony in the prone position as compared to the supine position (35). Our results confirm that lateral position may lead to a redistribution of ventilation towards the dependent lung areas in neonates. One possible explanation for this seemingly paradoxical behavior could be provided by the underlying disease physiology: The redistribution of ventilation towards the dependent lung with lateral positioning occurred mainly in neonates with RDS (supplementary table S2). Moreover, the subgroup with RDS did not exhibit the redistribution of ventilation towards the dorsal (non-

ANNALSATS Articles in Press. Published December 13, 2021 as 10.1513/AnnalsATS.202005-562OC

dependent) lung during prone positioning that was observed in infants without RDS (supplementary table S1). We speculate that the different mechanical properties of the lungs of neonates suffering from RDS led to a relative overdistension of the non-dependent lung, resulting in a redistribution of ventilation towards the dependent lung in these patients.

**Assessment of overall degree of ventilation inhomogeneity with EIT**

Ventilation inhomogeneity as assessed by the GI index and the coefficient of variation increased in the prone position (as compared to the supine position) and in the right lateral position (as compared to the left lateral position). These increases in inhomogeneity were more pronounced in infants and children with PMA above 37 weeks in comparison to premature infants with PMA below 37 weeks. This may indicate the more pronounced effect of gravity on the background of chest growth.

The subgroup of patients with RDS showed a significantly different response to prone positioning in terms of ventilation inhomogeneity: in this subgroup, prone positioning decreased the GI index, indicating a more homogeneous ventilation distribution (supplementary table S1).

All EIT parameters used in this study are established measures quantitatively describing the ventilation distribution in the examined chest section and the overall degree of ventilation inhomogeneity. These measures were deemed clinically significant as previously assessed in a survey among 36 clinicians with previous experience with EIT (36). Both EIT measures of ventilation distribution and inhomogeneity were consistent throughout the study duration with no systematic changes (Table 2), indicating the robustness of these measurements.

ANNALSATS Articles in Press. Published December 13, 2021 as 10.1513/AnnalsATS.202005-562OC

**Limitations**

Our study has some limitations. With its purely observational design and the blinding of clinical researchers to EIT findings, the study was not suitable for demonstrating a clinical outcome benefit from continuous monitoring with EIT. The offline analysis of posture changes and clinical findings depended on the quality of clinical documentation of these events using the graphical user interface. In some cases, erroneous documentation of findings or interventions occurred. To counteract this limitation, we used the video log to verify the exact timing of all documented interventions wherever possible. If, for example, a documented patient position could not be verified using the video log, it was not used for the analyses presented in this manuscript. We must acknowledge that the mixed population and the observational study design limit the relevance of the conducted analyses with respect to the future clinical use of EIT. Studies on more homogeneous groups of patients with clearly defined intervention are needed for that purpose.

The patient's skin condition was only checked routinely during patient care by the clinical staff and there was no specific protocol for skin evaluation during the study period. Therefore, minor skin irritations may have gone unnoticed. As all adverse events were noted manually on the paper-based case report form, there was no uniform definition of adverse events. The ultrasound gel that was used to improve the electrode-skin contact is not approved as EIT contact agent and due to the non-randomized study design, adverse events caused by its prolonged use cannot be entirely excluded. In the meantime, a dedicated neonatal EIT contact agent has been developed that is recommended by the manufacturer for use in children and neonates (NeoContactAgent®, Sentec, Landquart, Switzerland)."

ANNALSATS Articles in Press. Published December 13, 2021 as 10.1513/AnnalsATS.202005-562OC

Despite these limitations, this study provides, for the first time, evidence of feasibility and safety of prolonged bedside EIT monitoring of ventilation in a vulnerable population and under routine clinical conditions. This makes EIT an ideal and promising candidate for lung function monitoring in infants and children. The CRADL study has created a large database of EIT data in neonates and young children with respiratory failure, with more than 10,000 hours of EIT recordings comprising more than 1.5 Billion EIT images. This database is open for methodological research and can be used to generate hypotheses for clinical studies as well as for development and evaluation of advanced methods of EIT image reconstruction and EIT data analysis.

**Conclusion**

In conclusion, our observational study shows the feasibility and safety of continuous EIT monitoring for up to 72 hours in a large group of neonates and young children with or at risk for respiratory failure. We found no major adverse effects and demonstrated that EIT can be used to track changes in ventilation distribution in a routine clinical setting. Future studies of EIT in the neonatal population should use unblinded EIT images and focus on early detection of adverse events and on guiding ventilator therapy with online measurements of EIT.

ANNALSATS Articles in Press. Published December 13, 2021 as 10.1513/AnnalsATS.202005-562OC

## References


1. Frerichs I, Amato MB, van Kaam AH, Tingay DG, Zhao Z, Grychtol B, Bodenstein M, Gagnon H, Böhm SH, Teschner E, Stenqvist O, Mauri T, Torsani V, Camporota L, Schibler A, Wolf GK, Gommers D, Leonhardt S, Adler A; TREND study group. Chest electrical impedance tomography examination, data analysis, terminology, clinical use and recommendations: consensus statement of the TRanslational EIT development stuDy group. Thorax. 2017 Jan;72(1):83-93. doi: 10.1136/thoraxjnl-2016-208357.
2. Riedel T, Frerichs I. Electrical impedance tomography. Eur Respir Mon 2010; 47:195-205
3. Wolf GK, Gómez-Laberge C, Kheir JN, Zurakowski D, Walsh BK, Adler A, Arnold JH. Reversal of dependent lung collapse predicts response to lung recruitment in children with early acute lung injury. Pediatr Crit Care Med. 2012 Sep;13(5):509-15. doi: 10.1097/PCC.0b013e318245579c.
4. Bhatia R, Davis PG, Tingay DG. Regional Volume Characteristics of the Preterm Infant Receiving First Intention Continuous Positive Airway Pressure. J Pediatr. 2017 Aug;187:80-88.e2. doi: 10.1016/j.jpeds.2017.04.046.
5. Wolf GK, Gómez-Laberge C, Rettig JS, Vargas SO, Smallwood CD, Prabhu SP, Vitali SH, Zurakowski D, Arnold JH. Mechanical ventilation guided by electrical impedance tomography in experimental acute lung injury. Crit Care Med. 2013 May;41(5):1296-304. doi: 10.1097/CCM.0b013e3182771516.
6. Rossi FdS, Yagui AC, Haddad LB, Deutsch AD, Rebello CM. Electrical impedance tomography to evaluate air distribution prior to extubation in very-low-birth-weight infants: a feasibility study. Clinics (Sao Paulo). 2013;68(3):345-50.
7. Miedema M, de Jongh FH, Frerichs I, van Veenendaal MB, van Kaam AH. Changes in lung volume and ventilation during lung recruitment in high-frequency ventilated preterm infants with respiratory distress syndrome. J Pediatr. 2011 Aug;159(2):199-205.e2. doi: 10.1016/j.jpeds.2011.01.066.
8. Frerichs I, Schiffmann H, Hahn G, Hellige G. Non-invasive radiation-free monitoring of regional lung ventilation in critically ill infants. Intensive Care Med. 2001 Aug;27(8):1385-94.
9. Heinrich S, Schiffmann H, Frerichs A, Klockgether-Radke A, Frerichs I. Body and head position effects on regional lung ventilation in infants: An electrical impedance tomography study. Intensive Care Med. 2006 Sep;32(9):1392-8.
10. Hough JL, Johnston L, Brauer SG, Woodgate PG, Pham TM, Schibler A. Effect of body position on ventilation distribution in preterm infants on continuous positive airway pressure. Pediatr Crit Care Med. 2012 Jul;13(4):446-51. doi:10.1097/PCC.0b013e31822f18d9.
11. van der Burg PS, Miedema M, de Jongh FH, Frerichs I, van Kaam AH. Changes in lung volume and ventilation following transition from invasive to noninvasive respiratory


ANNALSATS Articles in Press. Published December 13, 2021 as 10.1513/AnnalsATS.202005-562OC

support and prone positioning in preterm infants. Pediatr Res. 2015 Mar;77(3):484-8. doi: 10.1038/pr.2014.201.

12. Hough J, Trojman A, Schibler A. Effect of time and body position on ventilation in premature infants. Pediatr Res. 2016 Oct;80(4):499-504. doi:10.1038/pr.2016.116.
13. van der Burg PS, de Jongh FH, Miedema M, Frerichs I, van Kaam AH. The effect of prolonged lateral positioning during routine care on regional lung volume changes in preterm infants. Pediatr Pulmonol. 2016 Mar;51(3):280-5. doi:10.1002/ppul.23254
14. Miedema M, de Jongh FH, Frerichs I, van Veenendaal MB, van Kaam AH. Changes in lung volume and ventilation during surfactant treatment in ventilated preterm infants. Am J Respir Crit Care Med. 2011 Jul 1;184(1):100-5. doi: 10.1164/rccm.201103-0375OC.
15. Chatziioannidis I, Samaras T, Mitsiakos G, Karagianni P, Nikolaidis N. Assessment of lung ventilation in infants with respiratory distress syndrome using electrical impedance tomography. Hippokratia. 2013 Apr;17(2):115-9.
16. Kallio M, van der Zwaag AS, Waldmann AD, Rahtu M, Miedema M, Papadouri T, van Kaam AH, Rimensberger PC, Bayford R, Frerichs I. Initial Observations on the Effect of Repeated Surfactant Dose on Lung Volume and Ventilation in Neonatal Respiratory Distress Syndrome. Neonatology. 2019;116(4):385-389. doi:10.1159/000502612.
17. Bhatia R, Schmölzer GM, Davis PG, Tingay DG. Electrical impedance tomography can rapidly detect small pneumothoraces in surfactant-depleted piglets. Intensive Care Med. 2012 Feb;38(2):308-15. doi: 10.1007/s00134-011-2421-z.
18. Miedema M, Frerichs I, de Jongh FH, van Veenendaal MB, van Kaam AH. Pneumothorax in a preterm infant monitored by electrical impedance tomography: a case report. Neonatology. 2011;99(1):10-3. doi: 10.1159/000292626.
19. Miedema M, Adler A, McCall KE, Perkins EJ, van Kaam AH, Tingay DG. Electrical impedance tomography identifies a distinct change in regional phase angle delay pattern in ventilation filling prior to a spontaneous pneumothorax. J Appl Physiol (1985). 2019 Jul 3. doi: 10.1152/japplphysiol.00973.2018.
20. Rahtu M, Frerichs I, Waldmann AD, Strodthoff C, Becher T, Bayford R, Kallio M. Early Recognition of Pneumothorax in Neonatal RDS with Electrical Impedance Tomography. Am J Respir Crit Care Med. 2019 May 15. doi:10.1164/rccm.201810-1999IM. [Epub ahead of print] PubMed PMID: 31091957.
21. van der Burg PS, Miedema M, de Jongh FH, van Kaam AH. Unilateral atelectasis in a preterm infant monitored with electrical impedance tomography: a case report. Eur J Pediatr. 2014 Dec;173(12):1715-7. doi: 10.1007/s00431-014-2399-y.
22. Schmölzer GM, Bhatia R, Davis PG, Tingay DG. A comparison of different bedside techniques to determine endotracheal tube position in a neonatal piglet model. Pediatr Pulmonol. 2013 Feb;48(2):138-45. doi: 10.1002/ppul.22580.

ANNALSATS Articles in Press. Published December 13, 2021 as 10.1513/AnnalsATS.202005-562OC

23. Steinmann D, Engehausen M, Stiller B, Guttmann J. Electrical impedance tomography for verification of correct endotracheal tube placement in paediatric patients: a feasibility study. Acta Anaesthesiol Scand. 2013 Aug;57(7):881-7. doi: 10.1111/aas.12143.
24. Armstrong RK, Carlisle HR, Davis PG, Schibler A, Tingay DG. Distribution of tidal ventilation during volume-targeted ventilation is variable and influenced by age in the preterm lung. Intensive Care Med. 2011 May;37(5):839-46. doi: 10.1007/s00134-011-2157-9.
25. Sophocleous L, Frerichs I, Miedema M, Kallio M, Papadouri T, Karaoli C, Becher T, Tingay DG, van Kaam AH, Bayford R, Waldmann AD. Clinical performance of a novel textile interface for neonatal chest electrical impedance tomography. Physiol Meas. 2018 Apr 26;39(4):044004. doi: 10.1088/1361-6579/aab513.
26. Adler A, Arnold JH, Bayford R, Borsic A, Brown B, Dixon P, Faes TJ, Frerichs I, Gagnon H, Gärber Y, Grychtol B, Hahn G, Lionheart WR, Malik A, Patterson RP, Stocks J, Tizzard A, Weiler N, Wolf GK. GREIT: a unified approach to 2D linear EIT reconstruction of lung images. Physiol Meas. 2009, 30(6):S35-55.
27. Khodadad D, Nordebo S, Müller B, Waldmann A, Yerworth R, Becher T, Frerichs I, Sophocleous L, van Kaam A, Miedema M, Seifnaraghi N, Bayford R. Optimized breath detection algorithm in electrical impedance tomography. Physiol Meas. 2018, 39(9):094001. doi: 10.1088/1361-6579/aad7e6.
28. Zhao Z, Möller K, Steinmann D, Frerichs I, Guttmann J. Evaluation of an electrical impedance tomography-based Global Inhomogeneity Index for pulmonary ventilation distribution. Intensive Care Med. 2009 Nov;35(11):1900-6. doi: 10.1007/s00134-009-1589-y.
29. Becher T, Vogt B, Kott M, Schädler D, Weiler N, Frerichs I. Functional Regions of Interest in Electrical Impedance Tomography: A Secondary Analysis of Two Clinical Studies. PLoS One. 2016 Mar 24;11(3):e0152267. doi: 10.1371/journal.pone.0152267.
30. Thomson J, Rüegger CM, Perkins EJ, Pereira-Fantini PM, Farrell O, Owen LS, Tingay DG. Regional ventilation characteristics during non-invasive respiratory support in preterm infants. Arch Dis Child Fetal Neonatal Ed. 2021 Jul;106(4):370-375. doi: 10.1136/archdischild-2020-320449. Epub 2020 Nov 27.
31. Heaf DP, Helms P, Gordon I, Turner HM. Postural Effects on Gas Exchange in Infants. N Engl J Med 1983, 308(25):1505-8. doi: 10.1056/NEJM198306233082505.
32. Davies H, Kitchman R, Gordon I, Helms P. Regional ventilation in infancy. Reversal of adult pattern. N Engl J Med. 1985 Dec 26;313(26):1626-8. doi: 10.1056/NEJM198512263132603.
33. Lupton-Smith AR, Argent AC, Rimensberger PC, Morrow BM. Challenging a paradigm: positional changes in ventilation distribution are highly variable in healthy infants and children. Pediatr Pulmonol. 2014 Aug;49(8):764-71. doi: 10.1002/ppul.22893.

ANNALSATS Articles in Press. Published December 13, 2021 as 10.1513/AnnalsATS.202005-562OC

34. Rehan VK, Nakashima JM, Gutman A, Rubin LP, McCool FD. Effects of the supine and prone position on diaphragm thickness in healthy term infants. Arch Dis Child. 2000 Sep;83(3):234-8. doi: 10.1136/adc.83.3.234.
35. Wolfson MR, Greenspan JS, Deoras KS, Allen JL, Shaffer TH. Effect of position on the mechanical interaction between the rib cage and abdomen in preterm infants. J Appl Physiol (1985). 1992 Mar;72(3):1032-8. doi: 10.1152/jappl.1992.72.3.1032.
36. Frerichs I, Becher T. Chest electrical impedance tomography measures in neonatology and paediatrics-a survey on clinical usefulness. Physiol Meas. 2019 Jun 4;40(5):054001. doi: 10.1088/1361-6579/ab1946.

ANNALSATS Articles in Press. Published December 13, 2021 as 10.1513/AnnalsATS.202005-562OC

**Table 1.** Respiratory support and oxygenation at beginning and end of study duration.

| Mode / Parameter | Start of study | End of study * |
|---|---|---|
| **Invasive ventilation (n)** | 55 | 24 |
| **HFNC (n)** | 62 | 73 |
| **nCPAP (n)** | 70 | 47 |
| **NIPPV (n)** | 8 | 8 |
| **NIV-NAVA (n)** | 2 | 3 |
| **LFNO / no support (n)** | 3 | 39 |
| **$FiO_2$** | 0.28±0.12 | 0.25±0.11 |
| **$SpO_2$ (%)** | 94±4 | 95±5 |

* In six cases, the mode of respiratory support at the end of study was not documented. HFNC = high flow nasal cannula; nCPAP = nasal continuous positive airway pressure; NIPPV = nasal intermittent positive pressure ventilation; NIV-NAVA = non-invasive neurally adjusted ventilatory assist; LFNO = low-flow nasal oxygen; $FiO_2$ = fraction of inspired oxygen; $SpO_2$ = arterial oxygen saturation by pulse oxymetry.

ANNALSATS Articles in Press. Published December 13, 2021 as 10.1513/AnnalsATS.202005-562OC

**Table 2.** Summary of EIT parameters obtained in the study population over the study duration.

| **Ventilation distribution** | **Baseline** | **12 h** | **24 h** | **36 h** | **48 h** | **60 h** | **End of study** |
|---|---|---|---|---|---|---|---|
| %right / %left (±SD) | 56 / 44 (±14) | 57 / 43 (±15) | 58 / 42 (±15) | 57 / 43 (±16) | 59 / 41 (±15) | 59 / 41 (±16) | 58 / 42 (±15) |
| %ventral / %dorsal (±SD) | 43 / 57 (±10) | 42 / 58 (±12) | 41 / 59 (±11) | 41 / 59 (±12) | 40 / 60 (±10) | 42 / 58 (±12) | 42 / 58 (±11) |
| GI Index [IQR] | 1.29 [1.22-1.47] | 1.32 [1.22-1.63] | 1.32 [1.22-1.6] | 1.36 [1.22-1.68] | 1.3 [1.21-1.73] | 1.32 [1.2-1.67] | 1.34 [1.22-1.68] |
| CV [IQR] | 2 [1.84-2.36] | 2.07 [1.84-2.55] | 2.07 [1.82-2.54] | 2.1 [1.86-2.59] | 2.09 [1.85-2.64] | 2.13 [1.8-2.44] | 2.08 [1.84-2.63] |
| **Patient position** | | | | | | | |
| Supine (%) | 83 | 51.1 | 50 | 45.2 | 45.4 | 42.9 | 53.5 |
| Prone (%) | 6.5 | 13.8 | 14.3 | 14.8 | 10.9 | 9.2 | 13.1 |
| Left lateral (%) | 4.5 | 15.4 | 17.9 | 20.6 | 22.7 | 25.5 | 16.7 |
| Right lateral (%) | 6.0 | 19.7 | 17.9 | 19.4 | 21.0 | 22.4 | 16.7 |
| | | | | | | | |
| **N** | **200** | **191** | **186** | **155** | **134** | **99** | **200** |

Parametric values are presented as mean ± standard deviation, non-parametric values are presented as median and interquartile range [IQR]. Note that “end of study” denotes the end of the study duration for each patient individually, and is therefore not identical with 72 hours in many patients. %dorsal / %ventral = percentage of ventilation in the dorsal / ventral hemithorax. %right / %left = percentage of ventilation in the right / left hemithorax. GI index = global inhomogeneity index. CV = coefficient of variation. N = number of patient datasets contributing to each time point listed.

ANNALSATS Articles in Press. Published December 13, 2021 as 10.1513/AnnalsATS.202005-562OC

**Table 3.** Effect of supine vs. prone positioning on EIT parameters.

| EIT Parameter | Supine (whole study population, (n=179)) | Prone (whole study population, (n=87)) | Supine (PMA < 37 weeks, (n=143) | Prone (PMA < 37 weeks, n=77) | Supine (PMA ≥ 37 weeks, n=36) | Prone (PMA ≥ 37 weeks, n=10) |
|---|---|---|---|---|---|---|
| **%dorsal** (± SD) | 58* (± 17.1) | 63* (± 16.7) | 59* (± 16.9) | 63* (± 16.7) | 55* (± 18) | 64* (± 17.1) |
| %right (± SD) | 65* (± 21) | 62* (± 24.1) | 64 (± 21.1) | 62 (± 23.9) | 68 (± 20.1) | 62 (± 26.1) |
| **GI Index** [IQR] | 1.45* [1.30-1.74] | 1.54* [1.31-1.86] | 1.46 [1.30-1.78] | 1.51 [1.30-1.86] | 1.42* [1.28-1.63] | 1.74* [1.43-1.84] |
| **CV** [IQR] | 2.21* [1.94-2.69] | 2.33* [1.98-2.81] | 2.22 [1.94-2.73] | 2.30 [1.96-2.8] | 2.17* [1.93-2.55] | 2.61* [2.35-2.84] |

GI index = global inhomogeneity index. CV = coefficient of variation. %dorsal = percentage of ventilation in the dorsal hemithorax. %right = percentage of ventilation in the right hemithorax. * = $p<0.05$ for comparison supine vs. prone position. %dorsal denotes the anatomically dorsal part of the lungs, which is dependent in supine position and non-dependent in prone position. Parametric values are presented as mean ± standard deviation, non-parametric values are presented as median and interquartile range [IQR].

ANNALSATS Articles in Press. Published December 13, 2021 as 10.1513/AnnalsATS.202005-562OC

**Table 4.** Effect of left vs. right lateral positioning on EIT parameters.

| **EIT Parameter** | **Left lateral** (whole study population, n=180) | **Right lateral** (whole study population, n=180) | **Left lateral** (PMA < 37 weeks, n=144) | **Right lateral** (PMA < 37 weeks, n=142) | **Left lateral** (PMA ≥ 37 weeks, n=36) | **Right lateral** (PMA ≥ 37 weeks, n=38) |
|---|---|---|---|---|---|---|
| **%dorsal** (± SD) | 58$^{\$}$ (± 16.8) | 60$^{\$}$ (± 17.1) | 59$^{\$}$ (± 16.5) | 61$^{\$}$ (± 16.9) | 56 (± 17.9) | 58 (± 17.7) |
| **%right** (± SD) | 64 (± 22.1) | 65 (± 23.2) | 62$^{\$}$ (± 21.7) | 66$^{\$}$ (± 22.7) | 70$^{\$}$ (± 22.2) | 63$^{\$}$ (± 24.6) |
| **GI Index** [IQR] | 1.37$^{\$}$ [1.27-1.59] | 1.44$^{\$}$ [1.29-1.75] | 1.38$^{\$}$ [1.27-1.59] | 1.43$^{\$}$ [1.29-1.75] | 1.36$^{\$}$ [1.27-1.56] | 1.46$^{\$}$ [1.3-1.73] |
| **CV** [IQR] | 2.10$^{\$}$ [1.90-2.46] | 2.24$^{\$}$ [1.97-2.73] | 2.08$^{\$}$ [1.89-2.44] | 2.22$^{\$}$ [1.97-2.73] | 2.16$^{\$}$ [1.94-2.53] | 2.28$^{\$}$ [1.98-2.72] |

GI index = global inhomogeneity index. CV = coefficient of variation. %dorsal = percentage of ventilation in the dorsal hemithorax. %right = percentage of ventilation in the right hemithorax. $^{\$}$ = $p<0.05$ for comparison left lateral vs. right lateral position. Parametric values are presented as mean ± standard deviation, non-parametric values are presented as median and interquartile range

ANNALSATS Articles in Press. Published December 13, 2021 as 10.1513/AnnalsATS.202005-562OC

**Figure legends**

**Figure 1.** EIT device with study-specific graphical user interface (GUI) in a clinical intensive care unit setting. The GUI allows documentation of patient position in angles of 45° and displays color-coded bars indicating the quality of regional electrode contact impedance, real-time documentation of clinical findings and interventions as well as basic patient data and the video stream that was used for offline verification of clinically documented events. Background: Infant with EIT belt placed around the chest circumference at the level of the 5$^{th}$ intercostal space.

**Figure 2.** EIT images displaying ventilation distribution in two exemplary infants in different body positions. Black and grey color indicate areas with low tidal impedance change, whereas purple color indicates areas with higher tidal impedance change. **Panels A+B:** Ventilation distribution in a neonate aged 29 weeks (postmenstrual age) suffering from respiratory distress syndrome treated with high flow nasal cannula oxygen in the supine (A) and in the prone position (B). **Panels C+D:** Ventilation distribution in an infant aged 43 weeks (postmenstrual age) intubated for laryngomalacia undergoing pressure-controlled ventilation in the left (C) and right lateral position (D). Abbreviations: a = anterior; p = posterior; r = right; l = left.

**Figure 3.** Flow diagram reporting number of patients (n) screened, included, overall duration of electrical impedance tomography (EIT) recordings and the reasons for termination of EIT recordings before 72 hours had expired.

ANNALSATS Articles in Press. Published December 13, 2021 as 10.1513/AnnalsATS.202005-562OC


Figure 1. EIT device with study-specific graphical user interface (GUI) in a clinical intensive care unit setting. The GUI allows documentation of patient position in angles of 45° and displays color-coded bars indicating the quality of regional electrode contact impedance, real-time documentation of clinical findings and interventions as well as basic patient data and the video stream that was used for offline verification of clinically documented events. Background: Infant with EIT belt placed around the chest circumference at the level of the 5th intercostal space.

200x133mm (200 x 200 DPI)

ANNALSATS Articles in Press. Published December 13, 2021 as 10.1513/AnnalsATS.202005-562OC

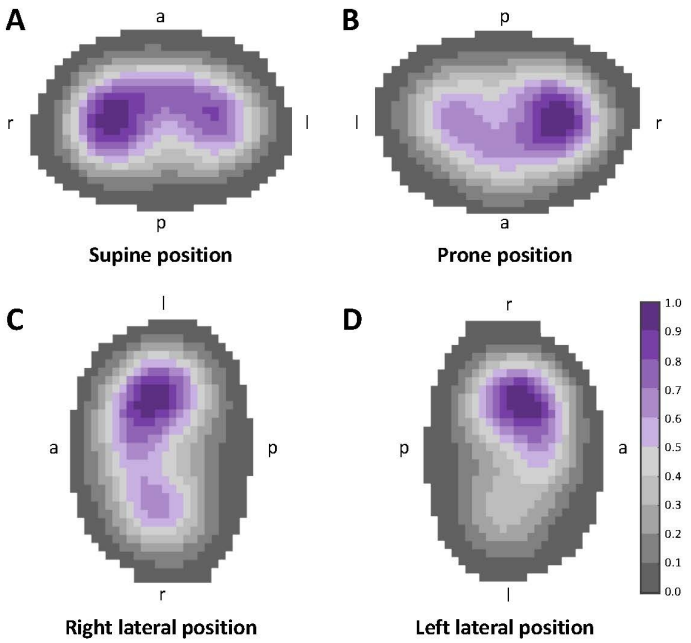


Figure 2. EIT images displaying ventilation distribution in two exemplary infants in different body positions. Black and grey color indicate areas with low tidal impedance change, whereas purple color indicates areas with higher tidal impedance change. Panels A+B: Ventilation distribution in a neonate aged 29 weeks (postmenstrual age) suffering from respiratory distress syndrome treated with high flow nasal cannula oxygen in the supine (A) and in the prone position (B). Panels C+D: Ventilation distribution in an infant aged 43 weeks (postmenstrual age) intubated for laryngomalacia undergoing pressure-controlled ventilation in the left (C) and right lateral position (D). Abbreviations: a = anterior; p = posterior; r = right; l = left.

190x142mm (220 x 220 DPI)

ANNALSATS Articles in Press. Published December 13, 2021 as 10.1513/AnnalsATS.202005-562OC

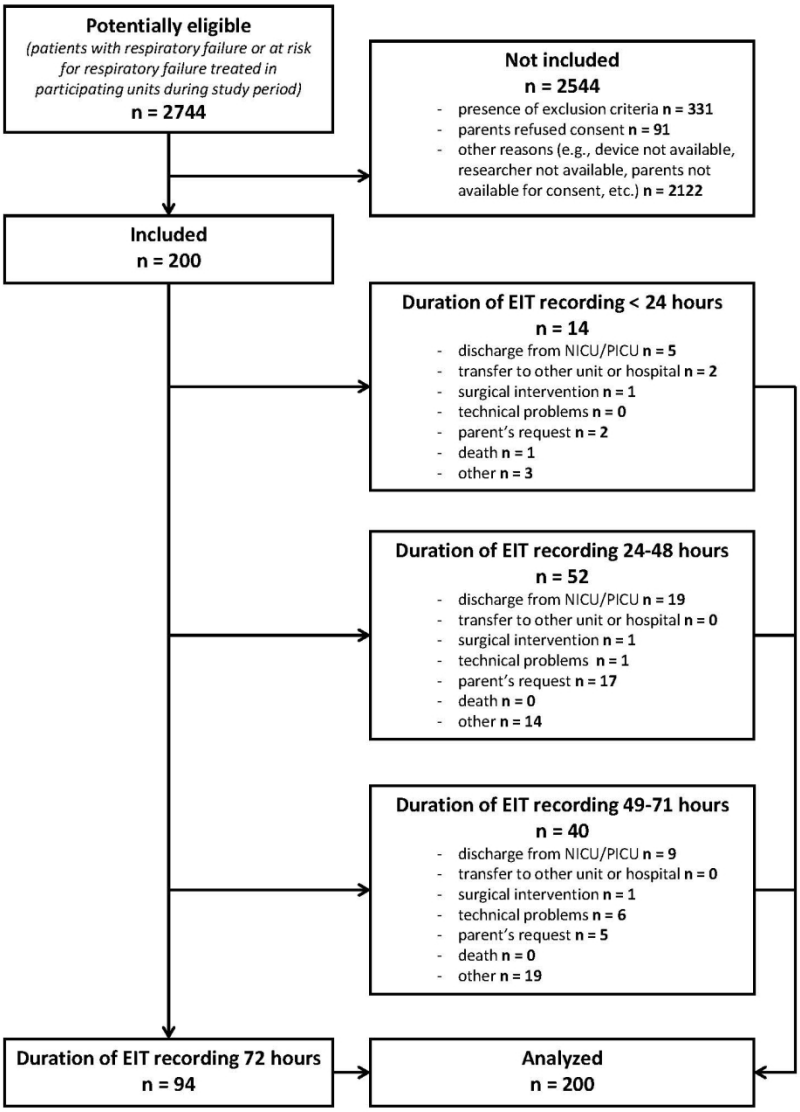


Figure 3. Flow diagram reporting number of patients (n) screened, included, overall duration of electrical impedance tomography (EIT) recordings and the reasons for termination of EIT recordings before 72 hours had expired.

190x275mm (200 x 200 DPI)

ANNALSATS Articles in Press. Published December 13, 2021 as 10.1513/AnnalsATS.202005-562OC

# Online supplement

## Prolonged Continuous Monitoring of Regional Lung Function in Infants with Respiratory Failure

Tobias H. Becher (1); Martijn Miedema (2); Merja Kallio (3); Thalia Papadouri (4); Christina Karaoli (4); Louiza Sophocleous (5); Marika Rahtu (3); Ruud W. van Leuteren (2); Andreas D. Waldmann (6,11); Claas Strodthoff (1); Rebecca Yerworth (7); Antoine Dupré (8); Mohamed-Rida Benissa (8); Sven Nordebo (9); Davood Khodadad (9); Richard Bayford (10); Roseanne Vliegenthart (2); Peter C. Rimensberger (8); Anton H. van Kaam (2); Inéz Frerichs (1)

1) Dept. of Anesthesiology and Intensive Care Medicine, University Medical Center Schleswig-Holstein, Campus Kiel, Germany
2) Dept. of Neonatology, Emma Children's Hospital, Amsterdam University Medical Centers, University of Amsterdam and Vrije Universiteit Amsterdam, Amsterdam, Netherlands
3) PEDEGO Research Unit, Medical Research Center Oulu, University of Oulu, and Dept. of Children and Adolescents, Oulu University Hospital, Oulu, Finland
4) Dept. of Neonatology, Archbishop Makarios III Hospital, Nicosia, Cyprus
5) Dept. of Electrical and Computer Engineering, University of Cyprus, Nicosia, Cyprus
6) SenTec AG (formerly Swisstom AG), Landquart, Switzerland
7) Dept. of Medical Physics and Biomedical Engineering, University College London, United Kingdom;
8) Pediatric and Neonatal Intensive Care Unit, Children's Hospital, University of Geneva, Switzerland
9) Dept. of Physics and Electrical Engineering, Linnaeus University, Växjö, Sweden
10) Dept. of Natural Sciences, Middlesex University, London, United Kingdom
11) Department of Anesthesiology and Intensive Care Medicine, Rostock University Medical Center, Rostock, Germany

This online supplement contains additional information on electrical impedance tomography (EIT) data acquisition and EIT data analysis during the Continuous Regional Analysis Device for neonate Lungs (CRADL) observational study.

ANNALSATS Articles in Press. Published December 13, 2021 as 10.1513/AnnalsATS.202005-562OC

## EIT data acquisition

EIT data were acquired at a sampling rate of 48 images per second using a modified version of the SenTec BB$^2$ EIT system with non-adhesive textile 32-electrode belts for neonatal and pediatric use (SenTec AG (formerly Swisstom AG), Landquart, Switzerland) (1). EIT belts were available in six different sizes (17.5 cm, 20 cm, 23.5 cm, 27.5 cm, 33 cm and 44 cm) and were selected according to the individual patient's chest circumference.

Commonly used neonatal ultrasound gel (Aquasonic 100, Parker Laboratory Inc, USA) was applied to the belt before fastening along the 5–6th intercostal space. The skin contact quality was displayed on the EIT device's study-specific graphical user interface (GUI) throughout the duration of the study. According to the study protocol, gel was reapplied at least once in 24 h with a maximum of four reapplications of gel per day if skin contact was insufficient and more than six electrodes failed.

The EIT device's study-specific graphical user interface (GUI) provided online information on the quality of electrode-skin contact impedance (main manuscript, Figure 1, left) to allow reattaching the belt or reapplying the ultrasound gel if necessary.

A video camera was placed on the incubator to allow offline verification of events documented using the study GUI.

## EIT image reconstruction and data analysis

EIT image reconstruction is a multi-step process, the first (and arguably most important) step being acquisition of voltage differences with electrodes placed around the patient's chest circumference. The Sentec BB$^2$ device can perform image reconstruction whenever at least 26 out of 32 electrodes exhibit skin contact impedance of < 700 Ohm. When this criterion was fulfilled, image reconstruction was performed according to the well-established and validated Graz Consensus Reconstruction Algorithm for EIT (GREIT). Data analysis was performed after importing the reconstructed EIT images and saving the unfiltered data in Matlab. In a first step, EIT image data were filtered using a Bandpass filter with cutoff frequencies of 0.15 and 1.8 Hz. The image sum signal was calculated using all pixels within the thorax region. Individual breaths as well as respiratory rate were detected on the global impedance signal (representing the sum of all image pixels) with a breath detection algorithm optimized for neonates and young infants (3). Tidal images were generated for every detected breath by calculating the difference between impedance distribution at the end of inspiration and impedance distribution at start of inspiration. Tidal images recorded during unstable periods with more than six failing electrodes and during compensation events (i.e. internal recalibration of the EIT device to compensate for a change in the number of failing electrodes) were excluded from the data analysis. For all patients, the EIT examination time that was not excluded from the analysis was summed up and divided by the total examination time to assess the percentage of EIT examination time suitable for analyzing, which is reported as primary endpoint in the main manuscript.

## GI index and CV

GI Index parameters were calculated using all image pixels within the thorax region. Ventilation inhomogeneity was quantified with the global inhomogeneity index (GI index (4)) and the coefficient of variation (CV, 5). These calculations were performed on tidal images, where each pixel value represents the impedance difference (tidal variation, TV) between inspiration and the preceding

ANNALSATS Articles in Press. Published December 13, 2021 as 10.1513/AnnalsATS.202005-562OC

expiration. The GI index was calculated by calculating the median TV from all image pixels (Median($TV_{lung}$). Then for each image pixel, the amount of the difference from the median was calculated. The amounts were summed up and divided by the sum of all image pixels as described in (4):

$$GI = \sum_{l \in lung} \left| TV_l - Median(TV_{lung}) \right| \Big/ \sum_{l \in lung} TV_l$$

Higher values of GI index denote a higher inhomogeneity within the tidal image, with larger deviations in TV from the median value.

The CV was calculated by calculating the ratio between the standard deviation of TV and the mean TV using all tidal image pixels, with higher values denoting higher inhomogeneity within the tidal image. While GI index and CV are both measures of ventilation inhomogeneity, they differ in that GI index is based on deviations from the median TV (a non-parametric measure), while CV is based on the ratio between standard deviation and mean.

## Ventilation distribution

Ventrodorsal and right-to-left ventilation distributions were assessed by calculating the ventral and dorsal fraction of ventilation (%ventral, %dorsal) as well as the right-sided and left-sided percentage of ventilation (%right, %left) including all image pixels within the thorax region.

For calculating %ventral and %dorsal, the EIT image was split at one horizontal line in the middle of the anteroposterior thorax diameter and % ventral/dorsal were calculated as the sum of tidal impedance changes within the ventral/dorsal half of the image divided by the sum of tidal impedance changes in the whole EIT image multiplied by 100. Accordingly, for calculation of %right/%left, the EIT image was split at one vertical line in the middle of the right-to-left thorax diameter and %right/%left were calculated as the sum of tidal impedance changes within the right/left half of the image divided by the sum of tidal impedance changes in the whole EIT image multiplied by 100.

## Treatment of image pixels displaying negative values

Image pixels displaying negative values (i.e. a decrease in impedance during inspiration) were set equal to zero for calculating ventilation distribution and CoV but were taken into account for calculation of GI index and CV.

## References (online supplement only)

1. Sophocleous L, Frerichs I, Miedema M, Kallio M, Papadouri T, Karaoli C, Becher T, Tingay DG, van Kaam AH, Bayford R, Waldmann AD. Clinical performance of a novel textile interface for neonatal chest electrical impedance tomography. Physiol Meas. 2018 Apr 26;39(4):044004. doi: 10.1088/1361-6579/aab513.
2. Adler A, Arnold JH, Bayford R, Borsic A, Brown B, Dixon P, Faes TJ, Frerichs I, Gagnon H, Gärber Y, Grychtol B, Hahn G, Lionheart WR, Malik A, Patterson RP, Stocks J, Tizzard A, Weiler

ANNALSATS Articles in Press. Published December 13, 2021 as 10.1513/AnnalsATS.202005-562OC

N, Wolf GK. GREIT: a unified approach to 2D linear EIT reconstruction of lung images. Physiol Meas. 2009, 30(6):S35-55.

3. Khodadad D, Nordebo S, Müller B, Waldmann A, Yerworth R, Becher T, Frerichs I, Sophocleous L, van Kaam A, Miedema M, Seifnaraghi N, Bayford R. Optimized breath detection algorithm in electrical impedance tomography. Physiol Meas. 2018, 39(9):094001. doi: 10.1088/1361-6579/aad7e6.
4. Zhao Z, Möller K, Steinmann D, Frerichs I, Guttmann J. Evaluation of an electrical impedance tomography-based Global Inhomogeneity Index for pulmonary ventilation distribution. Intensive Care Med. 2009 Nov;35(11):1900-6. doi: 10.1007/s00134-009-1589-y.
5. Becher T, Vogt B, Kott M, Schädler D, Weiler N, Frerichs I. Functional Regions of Interest in Electrical Impedance Tomography: A Secondary Analysis of Two Clinical Studies. PLoS One. 2016 Mar 24;11(3):e0152267. doi: 10.1371/journal.pone.0152267.

ANNALSATS Articles in Press. Published December 13, 2021 as 10.1513/AnnalsATS.202005-562OC

# Online supplement

## Prolonged Continuous Monitoring of Regional Lung Function in Infants with Respiratory Failure

Tobias H. Becher (1); Martijn Miedema (2); Merja Kallio (3); Thalia Papadouri (4); Christina Karaoli (4); Louiza Sophocleous (5); Marika Rahtu (3); Ruud W. van Leuteren (2); Andreas D. Waldmann (6,11); Claas Strodthoff (1); Rebecca Yerworth (7); Antoine Dupré (8); Mohamed-Rida Benissa (8); Sven Nordebo (9); Davood Khodadad (9); Richard Bayford (10); Roseanne Vliegenthart (2); Peter C. Rimensberger (8); Anton H. van Kaam (2); Inéz Frerichs (1)

1) Dept. of Anesthesiology and Intensive Care Medicine, University Medical Center Schleswig- Holstein, Campus Kiel, Germany
2) Dept. of Neonatology, Emma Children's Hospital, Amsterdam University Medical Centers, University of Amsterdam and Vrije Universiteit Amsterdam, Amsterdam, Netherlands
3) PEDEGO Research Unit, Medical Research Center Oulu, University of Oulu, and Dept. of Children and Adolescents, Oulu University Hospital, Oulu, Finland
4) Dept. of Neonatology, Archbishop Makarios III Hospital, Nicosia, Cyprus
5) Dept. of Electrical and Computer Engineering, University of Cyprus, Nicosia, Cyprus
6) SenTec AG (formerly Swisstom AG), Landquart, Switzerland
7) Dept. of Medical Physics and Biomedical Engineering, University College London, United Kingdom;
8) Pediatric and Neonatal Intensive Care Unit, Children's Hospital, University of Geneva, Switzerland
9) Dept. of Physics and Electrical Engineering, Linnaeus University, Växjö, Sweden
10) Dept. of Natural Sciences, Middlesex University, London, United Kingdom
11) Department of Anesthesiology and Intensive Care Medicine, Rostock University Medical Center, Rostock, Germany

This online supplement contains additional information on changes in ventilation distribution and inhomogeneity with positioning according to the main underlying diagnosis.

ANNALSATS Articles in Press. Published December 13, 2021 as 10.1513/AnnalsATS.202005-562OC

| EIT Parameter | Supine | Prone | Supine | Prone | Supine | Prone | Supine | Prone |
|---|---|---|---|---|---|---|---|---|
| **Diagnosis** (n; PMA ±SD) | **Prematurity** (66, 31 ±2) | | **RDS** (78; 33 ±2.7) | | **Bronchiolitis** (6; 69±28) | | **BPD** (10; 39±8) | |
| **%dorsal** (± SD) | 61* (±16.5) | 64* (±16.2) | 59 (±16.9) | 61 (±14.8) | 42 (±19.4) | 45 (±9.0) | 62 (±14.2) | 68 (±25.2) |
| **%right** (± SD) | 65* (±22.8) | 60* (±23.9) | 64* (±20.5) | 72* (±18.1) | 65 (±18.2) | 68 (±24.9) | 62 (±24.3) | 60 (±22.5) |
| **GI Index** [IQR] | 1.56 [1.36-1.91] | 1.55 [1.31-1.83] | 1.43* [1.29-1.73] | 1.35* [1.2-1.55] | 1.66 [1.42-2.16] | 1.42 [1.39-1.44] | 1.72 [1.48-2.71] | 2.05 [1.86-3.3] |
| **CV** [IQR] | 2.36 [2.07-2.83] | 2.34 [1.98-2.78] | 2.17 [1.91-2.66] | 2.11 [1.84-2.42] | 2.48 [2.21-3.2] | 2.21 [2.15-2.28] | 2.62 [2.21-3.99] | 3.02 [2.69-4.81] |

**Table S1. Effect of supine vs. prone positioning on EIT parameters according to underlying diagnosis.** Below each diagnosis, we list the number of patients included in the analysis (n) and the average postmenstrual age (PMA) and its standard deviation (SD). RDS = respiratory distress syndrome. BPD = bronchopulmonary dysplasia. GI index = global inhomogeneity index. CV = coefficient of variation. %dorsal = percentage of ventilation in the dorsal hemithorax. * = $p<0.05$ for comparison supine vs. prone position. %right = percentage of ventilation in the right hemithorax. %dorsal denotes the anatomically dorsal part of the lungs, which is dependent in supine position and non-dependent in prone position. Parametric values are presented as mean ± standard deviation, non-parametric values are presented as median and interquartile range [IQR].

ANNALSATS Articles in Press. Published December 13, 2021 as 10.1513/AnnalsATS.202005-562OC

| EIT Parameter | Left lateral | Right lateral | Left lateral | Right lateral | Left lateral | Right lateral | Left lateral | Right lateral |
|---|---|---|---|---|---|---|---|---|
| **Diagnosis** (n; PMA ±SD) | **Prematurity** (66, 31 ±2) | | **RDS** (78; 33 ±2.7) | | **Bronchiolitis** (6; 69±28) | | **BPD** (10; 39±8) | |
| **%dorsal** (± SD) | 59 (±15.6) | 61 16.2 | 59$ (±16.5) | 61$ (±17.1) | 49 (±21.5) | 49 (±18.7) | 65 (±10.7) | 65 (±22.4) |
| **%right** (± SD) | 64$ (±23.2) | 60$ (±23.3) | 61$ (±21.3) | 68$ (±22.4) | 80$ (±18.9) | 45$ (±24.1) | 62 (±19.7) | 66 (±24.6) |
| **GI Index** [IQR] | 1.41$ [1.29-1.62] | 1.51$ [1.33-1.89] | 1.36$ [1.26-1.57] | 1.41$ [1.28-1.69] | 1.59 [1.29-2.09] | 1.93 [1.43-2.37] | 1.55 [1.37-2.89] | 2.25 [1.69-4.29] |
| **CV** [IQR] | 2.20$ [1.95-2.55] | 2.30$ [2.01-2.87] | 2.06$ [1.88-2.39] | 2.20$ [1.97-2.68] | 2.53 [2.07-3.56] | 3.01 [2.21-3.64] | 2.26 [2.05-4.08] | 3.35 [2.5-6.22] |

**Table S2. Effect of left lateral vs. right lateral positioning on EIT parameters according to underlying diagnosis.** Below each diagnosis, we list the number of patients included in the analysis (n) and the average postmenstrual age (PMA) and its standard deviation (SD). RDS = respiratory distress syndrome. BPD = bronchopulmonary dysplasia. GI index = global inhomogeneity index. CV = coefficient of variation. %dorsal = percentage of ventilation in the dorsal hemithorax. %right = percentage of ventilation in the right hemithorax. %right denotes the anatomically right part of the lungs, which is dependent in right lateral position and non-dependent in left lateral position. $ = $p<0.05$ for comparison left lateral vs. right lateral position. Parametric values are presented as mean ± standard deviation, non-parametric values are presented as median and interquartile range [IQR].

ANNALSATS Articles in Press. Published December 13, 2021 as 10.1513/AnnalsATS.202005-562OC

| EIT Parameter | Supine | Prone | Left Lateral | Right Lateral | Supine | Prone | Left Lateral | Right Lateral |
|---|---|---|---|---|---|---|---|---|
| **Respiratory Support** (n; PMA mean ±SD) | **Non-Invasive** (145, 33 ±4.6) | | | | **Invasive** (55; 33 ±5.7) | | | |
| **%dorsal** (± SD) | 59 *# (±17) | 63 * (±17) | 58 $ (±16) | 61 $# (±17) | 55 # (±19) | 57 (±13) | 57 (±18) | 58 # (±18) |
| **%right** (± SD) | 65 * (±21) | 62 * (±24) | 64 (±22) | 64 # (±23) | 66 (±22) | 64 (±23) | 63 $ (±23) | 70 $# (±22) |
| **GI Index** [IQR] | 1.49 # [1.33-1.77] | 1.54 [1.31-1.86] | 1.41 $# [1.29-1.68] | 1.47 $# [1.32-1.81] | 1.31 # [1.22-1.56] | 1.44 [1.26-1.84] | 1.3 # [1.21-1.51] | 1.31 # [1.22-1.52] |
| **CV** [IQR] | 1.91 *# [1.49-2.37] | 1.98 * [1.6-2.57] | 1.72 $ [1.34-2.26] | 1.98 $# [1.5-2.43] | 1.75 # [1.3-2.16] | 2.27 [1.53-2.7] | 1.59 # [1.26-2.04] | 1.76 # [1.31-2.18] |

**Table S3. Effect of positioning and type of respiratory support on EIT parameters.** N = number of patients included in analysis. PMA = postmenstrual age. SD = standard deviation. GI index = global inhomogeneity index. CV = coefficient of variation. %dorsal = percentage of ventilation in the dorsal hemithorax. %right = percentage of ventilation in the right hemithorax. %dorsal denotes the anatomically dorsal part of the lungs, which is dependent in supine position and non-dependent in prone position. %right denotes the anatomically right part of the lungs, which is dependent in right lateral position and non-dependent in left lateral position. * = $p<0.05$ for comparison supine vs. prone position. $ = $p<0.05$ for comparison left lateral vs. right lateral position. # = $p<0.05$ for comparison invasive vs. non-invasive respiratory support. Parametric values are presented as mean ± standard deviation, non-parametric values are presented as median and interquartile range [IQR]. Parametric values are presented as mean ± standard deviation, non-parametric values are presented as median and interquartile range [IQR].

ANNALSATS Articles in Press. Published December 13, 2021 as 10.1513/AnnalsATS.202005-562OC